Inorganica Chimica Acta, 52 (1981) 191–196
©Elsevier Sequoia S.A., Lausanne – Printed in Switzerland

Spectroscopic, Structural and Photochemical Properties of Cu(I) Halide Adducts with *cis*- and *trans*-Crotonitrile.

Part II. Structural and Photochemical Properties of Crotonitrile·CuX Complexes

MICHÈLE BOLTE

Laboratoire de Photochimie, UER Sciences, Université de Clermont-Ferrand II, Les Cézeaux, B.P. 45, 24, Avenue des Landais, 63170 Aubière, France

and MICHEL MASSAUX

Laboratoire de Physique des Matériaux, UER Sciences, Université de Clermont-Ferrand II, Le Cézeaux, B.P. 45, 24, Avenue des Landais, 63170 Aubière, France

Received April 14, 1981

It has been shown, by means of vibrational spectra analysis (see Part I, in this issue) [1], that in the complex isolated from CuX–crotonitrile solutions, the ligand has exclusively the trans *configuration. A radiocrystallographic study of the complexes in the solid state was of interest for assessing this conclusion. Moreover, the observed isomerization, as described in Part I, induced the photochemical study of the crotonitrile·CuX complexes.*

Introduction

As reported in Part I, the complexes between metallic salts and nitriles appear to be intermediate compounds in reactions of nitriles. It has been necessary to know the nature of the bonds formed.

Results obtained in IR and Raman spectroscopy showed the complexation of Copper(I) with the nitrile group of *cis* or *trans* crotonitrile.

An X-ray structural investigation can show exactly the nature of bonds involved. Moreover, a photochemical investigation permits one to determine the influence of the various types of complexation on the ligand behaviour.

Experimental

Structural Part

Synthesis and Crystallographic Study

Crystals of CtN·CuX (CtN = crotonitrile, X = Cl, Br, I) were prepared, after purification of starting materials, as described in Part I [1], by dissolving CuX in CtN containing both isomers, at room temperature, in a dry box containing inert atmosphere. By slowly evaporating this solution under a stream of dried N_2, colourless, acicular crystals separate.

They are air or moisture sensitive, and easily decomposed by loss of nitrile: for X-ray studies, they were sealed in N_2-filled Lindemann glass capillaries, previously saturated with CtN vapour; under these precautions, single crystals were stable to X-ray exposure during measurements time, and showed no significant alteration after several days.

Chemical and thermogravimetric analysis (see Part I) led to the chemical formula C_6H_5N·CuX; the density was determined pycnometrically in C_6H_5X, X being the same as in the crystal species.

Weissenberg photographs, using CuK_α radiation (λ = 1.5418 Å) and precession photographs, with MoK_α (λ = 0.7109 Å), were used to determine crystal symmetry and rough unit-cell parameters, with X = Cl, Br, I. This preliminary study showed that the three compounds are *isostructural*. Single crystals of the compounds with Cl and Br were mounted on a CAD 4 Enraf–Nonius, PDP 8/M computer monitored diffractometer, using MoK_α radiation monochromatized by an oriented graphite crystal. (CtN·CuI crystals do not have sufficient diffraction quality for such measurements).

Accurate unit-cell parameters were obtained by a least-squares procedure using the setting angles of 25 reflections. The data are reported in Table I. For the three compounds, the conditions limiting possible reflections (h00:h = 2n; 0k0:k = 2n; 001:1 = 2 n) agree with space group $P2_12_12_1$. Elongation axis of the needles is [100]; the morphology of crystals shows faces of {010}, {001}, {011} forms.

X-ray Diffraction Data Collection and Reduction

This work has been made for X = Br only. Diffraction data were collected at 293 K from a well-formed

TABLE I. Experimental Physical and Crystallographic Data for CtN·CuX (X = Cl, Br, I).

Space group	X = Cl $P2_12_12_1$	X = Br $P2_12_12_1$	X = I* $P2_12_12_1$
a (Å)	3.855(7)	3.982(8)	4.21(2)
b (Å)	9.710(6)	9.786(4)	9.81(5)
c (Å)	15.407(13)	15.758(13)	15.93(16)
V (Å)	577(2)	614(2)	658(20)
Formula weight (Daltons)	166.08	210.54	257.53
D_{obs} (g cm^{-3})	1.90(5)	2.30(6)	2.6(1)
D_x (g cm^{-3})	1.912(7)	2.278(8)	2.60(8)
Z	4	4	4
μ_{MoK_α} (cm^{-1})	42.2	104.3	80.6

*Unit-cell parameters determination by photographic methods only.

single crystal; it was mounted with its [100] axis coïncident with the spindle axis on the four circle diffractometer CAD 4.

The radiation used was graphite monochromatized MoK_α ($\lambda = 0.71069$ Å). First, the mosaïcity of the crystal was examined by means of open counter ω scans at a take-off angle of 3°; the width at half-height for a typical strong low angle reflection (002) was 0.4°.

Intensities were measured up to $\theta_{max} = 40°$ ($0 \leqslant h \leqslant 6, 0 \leqslant k \leqslant 17, 0 \leqslant l \leqslant 28$) by ω–2θ scan mode.

Crystal–detector distance: 173 mm.

Detector window: Height: 4 mm; Width: 3.00 + 0.80 tgθ mm.

Prescan: Speed: 10° (min)$^{-1}$; SIGPRE = 0.20.

Scan angle: $\Delta\omega° = 1.25 + 0.35$ tgθ.

Scan time limited to ITMAX = 60 s.

Intensity measurement accuracy SIGMA = $\dfrac{\sigma(I)}{I}$ = 0.018.

Three standard reflections (200, 060, 0010) were monitored at regular intervals (3600 s) for both orientation and intensity controls. They showed only deviations from mean predicted by counting statistics.

2280 intensity data were collected in the reciprocal space range; but only 704 independent unique reflections with $I > 3\ \sigma$ (I) were corrected for Lorentz and polarization factors, and used to solve and refine the structure, after absorption correction. The shape of the crystal was assumed to be prismatic, limited by the three forms {010}, {001}, {011}; (the cross sections dimensions were 180, 260 and 350 μm). Crystal transmission factors were calculated and applied using the method proposed by De Meulenaer & Tompa [2].

Solution and Refinement of the Crystal Structure

In the space group $P2_12_12_1$, we must locate one Cu, one Br, one N and four C atoms (H atoms are neglected). The heavy atom method was used to solve the structure. Cu and Br atoms were first located by Patterson method, from (100) and (010) projections, then refined by full-matrix least-squares techniques [3], using 704 data. Scattering factors were from neutral atoms [4] corrected for dispersion [5].

Lighter atoms N and C were then located by Fourier difference maps. Their positions were introducted with isotropic thermal coefficients in the refinement.

The quantity minimized is $\Sigma W(|F_o| - |F_c|)^2$ were $|F_o|$ and $|F_c|$ are the observed and calculated structure amplitudes, put on the same scale, and the weight $W = 4F_o^2/\sigma^2(F_o^2)$. The reliability coefficients are defined as

$$R = (|F_o| - |F_c|)/\Sigma|F_o|$$

$$R_W = [\Sigma w(|F_o| - |F_c|)^2/\Sigma W F_o^2]^{1/2}$$

In the last cycle of refinement with isotropic thermal coefficients, R converged to 0.060; with anisotropic β_{ij} thermal coefficients (attenuation factor $\exp -(\beta_{11}h^2 + \beta_{22}k^2 + \beta_{33}l^2 + 2\beta_{12}hk + 2\beta_{23}kl + 2\beta_{13}lh)$), two refinement cycles led to final reliability factors R = 0.040 and R_W = 0.049 for the 704 observations and 64 variables.

The final positional and thermal parameters are listed in Table II; in this Table, organic atoms are listed N, C(0), C(1), C(2), C(3) with the numbering scheme

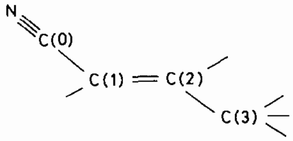

The listing of the final observed and calculated structure factors is available.

Photochemical Part (CuX = CuCl only)

Solutions of CuCl in *cis*- or *trans*-CtN were handled under inert atmosphere (dried N_2); the CuCl concentration is approximately 5×10^{-2} *M*. Degassing of the solutions was carried out by the usual freeze–pump–thaw method.

Irradiations at 253.7 nm were performed in a quartz reactor surrounded by six high intensity low pressure mercury lamps ($I_o \sim 2 \times 10^{16}$ photon cm^{-2} s^{-1}). The temperature remained constant at about 30 °C. Incident light intensity was measured using uranyl oxalate actinometry.

TABLE II. Final Atomic Parameters for CtN·CuBr (e.s.d'.s in parentheses).

Atom	x	y	z	β_{11}	β_{22}	β_{33}	β_{12}	β_{13}	β_{23}
Br	0.9507(4)	0.6651(2)	−0.0947(1)	0.046(1)	0.0104(1)	0.0037(1)	0.0013(5)	0.0000(3)	−0.0005(1)
Cu	0.4633(6)	0.6268(2)	−0.0013(1)	0.073(2)	0.0100(2)	0.0051(1)	0.0008(7)	−0.0011(4)	0.0013(1)
N	0.4108(41)	0.4523(13)	0.0556(8)	0.074(13)	0.0097(16)	0.0046(6)	0.0051(20)	0.0005(9)	−0.0002(5)
C(0)	0.3505(43)	0.3543(16)	0.0898(11)	0.083(15)	0.0087(20)	0.0048(8)	0.0008(22)	−0.0017(12)	−0.0008(7)
C(1)	0.2576(53)	0.2251(17)	0.1303(12)	0.084(15)	0.0090(21)	0.0056(9)	0.0049(23)	−0.0009(12)	0.0011(8)
C(2)	0.1440(47)	0.2232(17)	0.2069(10)	0.083(13)	0.0115(18)	0.0040(8)	0.0022(22)	−0.0003(10)	0.0008(7)
C(3)	0.0577(57)	0.0913(15)	0.2504(10)	0.091(17)	0.0075(16)	0.0042(7)	−0.0033(25)	0.0039(14)	0.0024(8)

Absorption spectra were recorded on a CARY 118 spectrometer. Samples were analysed either by VPC using a Carbowax 20 M column on a Carlo Erba Fractovap 2101 apparatus (the sum of both isomers is used as internal standard to calculate the percent of each isomer) or by infrared spectroscopy on a Perkin Elmer 180 ($\nu_{C=C}$ *cis* = 1625 cm^{-1}, $\nu_{C=C}$ *trans* = 1635 cm^{-1}) [1].

Results and Discussion

Structural Part

The structure is illustrated in Figs. 1 and 2, and selected significant bond distances and angles are given in Table III.

TABLE III. Interatomic Distances and Angles in *trans*-CtN·CuBr (e.s.d's. in parentheses).

Bond lengths (in Å)

Cu–Br	: 2.464(5)	N≡C(0)	: 1.126(20)
Cu–Br′	: 2.538(3)	C(0)–C(1)	: 1.464(24)
Cu–Br″	: 2.544(5)	C(1)=C(2)	: 1.289(25)
Cu←N	: 1.941(13)	C(2)–C(3)	: 1.500(22)

Bonds angles (in degrees)

Br–Cu–Br′	= 104.4(1)	Cu–Br–Cu′	= 77.4(1)
Br–Cu–Br″	= 105.3(2)	Cu–Br–Cu″	= 105.3(2)
Br′–Cu–Br″	= 102.2(1)	Cu′–Br–Cu″	= 76.0(1)
Br–Cu–N	= 119.6(5)	Cu–N–C(0)	= 173.7(16)
Br′–Cu–N	= 115.4(4)	N–C(0)–C(1)	= 176.6(19)
Br″–Cu–N	= 108.1(5)	C(0)–C(1)–C(2)	= 120.6(16)
		C(1)–C(2)–C(3)	= 121.3(15)

Figure 1 is the projection of the structure along [100]. This may be described in terms of infinite double chains of copper atoms connected by bridging Br (or X) atoms (Fig. 2). This structural scheme has been found in other R·CuX addition compounds [6]. CtN, in *trans*-configuration, is only complexed by N → Cu bonds.

Each copper atom is in *tetrahedral coordination* with three Br (X) atoms and one N atom. The Cu–Br distances are 2.464(5), 2.538(3) and 2.544(5) Å (standard value: 2.460(1) Å); the N → Cu bond length is 1.941(13) Å, similar to those observed in other analogous structures [7]. The X atom is coordinated with three copper atoms.

Within a chain, there are four-membered rings Cu_2Br_2 which are of particular interest because of the short Cu...Cu distance (3.127(4) Å), and the sharp Cu–Br–Cu angle (77.4(1)°) correlated with small, but significant distortions from regular tetrahedral coordination of the copper atom; these results suggest weak copper–copper interactions.

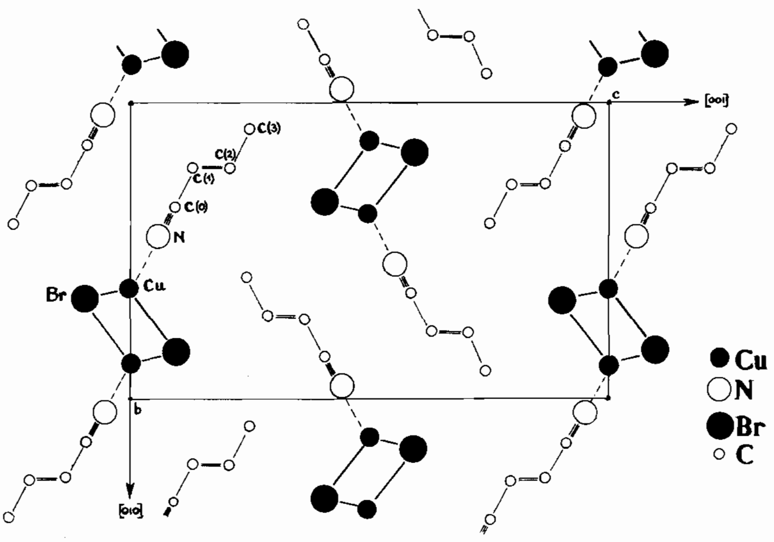

Fig. 1. Structure of *trans*-CtN•CuBr: Projection along [100].

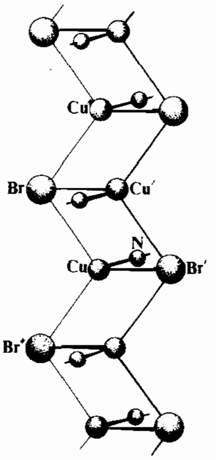

Fig. 2. Extension along [100] of a $(Cu_2Br_2)_\infty$ chain, showing Cu and Br coordination.

The geometry of the *trans*-CtN ligand molecule agrees with the classical data: N≡C: 1.158(4) Å; C=C: 1.337(6) Å; C–C: 1.44(1) Å [8].

A shortening of N≡C and C=C bond lengths may be caused by complexing through Cu ← N bonds. In a previous crystallographic study, one of us has reported the structure of MAN•CuBr (MAN = methacrylonitrile) [9].

The main structural scheme is quite different, but MAN molecules are also coordinated to Cu atoms by Cu ← N bonds. In this compound, we observed a similar shortening of N≡C, the other bond lengths being almost unmodified.

We have also described [10] the crystal structure of $AN \cdot Cu_2Cl_2$ (AN = acrylonitrile), in which the ligand coordination is assumed by both Cu ← N and $\mathrm{Cu}-\overset{\mathrm{C}}{\underset{\mathrm{C}}{\|}}$ metal olefin bonds. Then, N≡C and C–C bonds

TABLE IV. N≡C, C–C and C=C Bond Lengths (Å) in Pure or Coordinated Acrylonitrile, Methacrylonitrile and *trans*-Crotonitrile.

Nitrile		N≡C(0)	C(0)–C(1)	C(1)=C(2)
AN	pure	1.164(1)	1.426(1)	1.339(1)
	in $AN \cdot Cu_2Cl_2$	1.154(15)	1.442(15)	1.384(20)
MAN	pure	1.158(3)	1.442(7)	1.340(6)
	in MAN•CuBr	1.132(15)	1.440(18)	1.333(19)
trans-CtN	pure	1.158(4)	1.440(10)	1.337(6)
	in *trans*-CtN•CuBr	1.126(20)	1.464(24)	1.289(25)

in coordinated AN are almost unmodified, although C=C is elongated. Numerical data for comparison are shown in Table IV.

The *trans*-CtN ligand is *nearly planar.* We have determined, by least squares calculations, the 'best plane' for N, C(0), C(1), C(2), C(3) atoms. The plane equation is, in relative coordinates: $0.9322\ X + 0.0656\ Y - 0.3559\ Z = 0.0205$. Atom deviations, in Å, are: N: –0.009; C(0): 0.022; C(1): –0.013; C(2): –0.004; C(3): 0.004. The Cu atom, bonded to N, is –0.25 Å out of this plane.

A little, but significant distortion in the copper–ligand assembly can be pointed out: in the $Cu \leftarrow N\equiv C(0)–C(1)$ chain, we have found Cu–N–C(0) = 173.7 (16)°, N–C(0)–C(1) = 176.6 (19)°. This was observed in many other nitrile complexes [11].

Non bonding distances are in the expected range; the shortest Van Der Waals contacts are observed (Fig. 2) between Br and C(2) or C(3):

Br...C(2) = 3.684(18) Å
Br...C(3) = 3.842(17) Å

or between adjacent ligand molecules:

N...C(1) = 3.674(23) Å
C(0)...C(3) = 3.792(24) Å
C(2)...C(3) = 3.752(23) Å
N...C(3) = 3.833(23) Å

These attraction forces presume cohesive interactions between parallel $(Cu_2Br_2)_\infty$ chains.

Photochemical Part

The photosensitized isomerization of CtN is a well known phenomenon [12], but no quantitative results about direct photoisomerization have been reported. Thus, simultaneous studies on the pure crotonitriles and the CtN·CuCl complexes were performed. *Cis*- or *trans*-CtN are, both, the ligands with CuCl and the solvents for the obtained complexes.

Absorption Spectra

Complexes with *cis*- or *trans*-configuration of the ligand are obtained by dissolving CuCl in respectively *cis*- or *trans*-CtN. A difference spectrum comparing the spectrum of *cis*-CtN·CuCl complex with that of *cis*-CtN shows the specific transitions of the complex (Fig. 3).

$\lambda_{max} = 250$ nm and $\lambda_{max} = 280$ nm
$\epsilon = 8000\ M^{-1}\ cm^{-1}$ $\epsilon = 5500\ M^{-1}\ cm^{-1}$

The high-energy transition in the *trans*-CtN·CuCl complex cannot be observed precisely since the *trans*-CtN is highly absorbing, only the transition at longer wavelength can be determined.

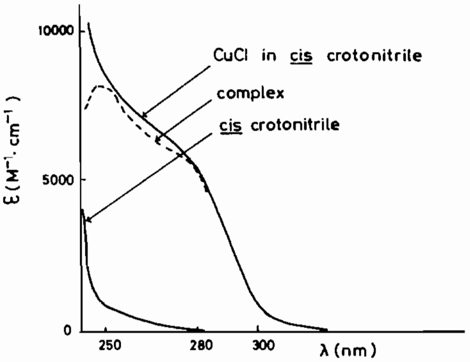

Fig. 3. Absorption spectrum of the *cis*-CtN·CuCl complex.

$\lambda_{max} = 280$ nm
$\epsilon = 4000\ M^{-1}\ cm^{-1}$

Photochemical Behaviour

By excitation at 254 nm of pure *cis*- or *trans*-CtN, low initial quantum yields of isomerization are measured (with 5% conversion):

$\phi^{o}_{t\to c} = 0.10 \pm 0.01$; $\phi^{o}_{c\to t} = 0.17 \pm 0.02$

By excitation at 254 nm of CtN·CuCl complex, the initial quantum yields are higher

$\phi^{o}_{t\to c} = 0.30 \pm 0.03$ $\phi^{o}_{c\to t} = 0.50 \pm 0.05$

The photoisomerization of *cis*-CtN by excitation at 254 nm of the *cis*-CtN complex is represented in Fig. 4. With CuCl concentration 5×10^{-2} *M* in *cis*-CtN, 30% of the solvent (~12 *M*) is transformed. Mass balance of the reaction shows the photoassistance of the *cis*–*trans* isomerization by the *cis*-CtN·CuCl complex.

The IR and Raman spectra indicate a complexation between the Cu atom and the C≡N group [1]; the crystal structure shows that the complexation involves the N atom of the nitrile group.

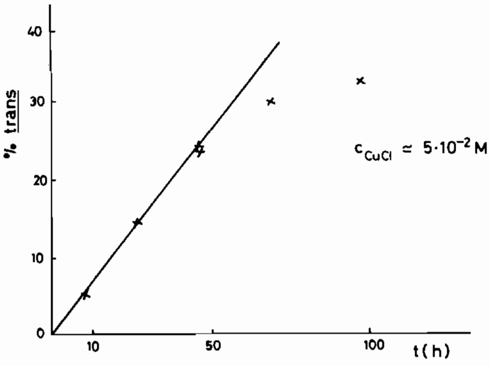

Fig. 4. Photoisomerization of the *cis*-crotonitrile in presence of CuCl ($\lambda_{irr.} = 254$ nm).

The photoassistance can be described as follows:

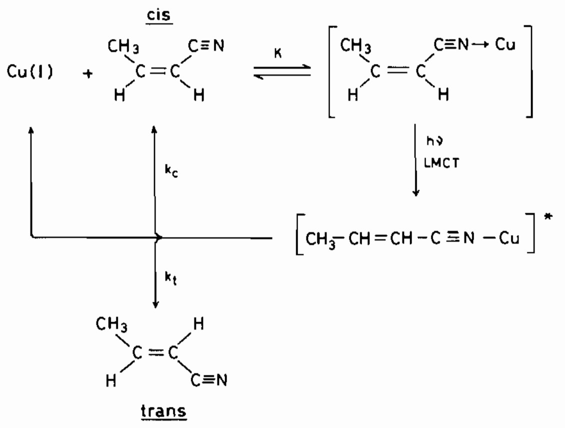

The results are analogous for the *trans*-isomer.

Remarks

The Raman spectra of *cis*-CtN complex in solution showed the presence of a very weak band at 1498 cm^{-1} which can be attributed to complexation between C=C and the Cu atom. This band only appears with the *cis*-isomer and cyclobutanic photodimerization is only observed from the *cis*-CtN·CuCl complex ($\phi_{\dim} = 6 \times 10^{-3}$).

We reported the same phenomenon with acrylonitrile and methacrylonitrile, which, by excitation of the CuCl complex, afforded cyclobutanic dimers [13].

References

1 J. Zarembowitch and M. Massaux, *Inorg. Chim. Acta*, (Part I, in this issue).
2 J. De Meulenaer and H. Tompa, *Acta Cryst.*, *19*, 1014 (1965).
3 W. R. Busing, K. O. Martin and H. A. Levy, ORFLS. Report ORNL-TM-305, Oak Ridge National Laboratory, Tennessee (1962).
4 D. T. Cromer and J. T. Waber, International Tables for X-Ray Crystallography, Vol. IV, Table 2.2A, p. 72 et sq., (1974).
5 D. T. Cromer, International Tables for X-Ray Crystallography, Vol. IV, Table 2.3.1, p. 149 (1974).
6 R = $\frac{1}{2}(C_2H_6N_2)$, X = Cl: I.D. Brown and J. D. Dunitz, *Acta Cryst.*, *13*, 28 (1960). R = CH_3CN, X = Cl: M. Massaux, M. J. Bernard and M. T. Le Bihan, *Bull. Soc. Fr. Miner. Crist.*, *92*, 118 (1969). R = CH_3CN, X = Br: M. Massaux, M. J. Bernard and M. T. Le Bihan, *Acta Cryst.*, *B27*, 2419 (1971). R = 3-Methylrhodanine, X = I: F. G. Moers, W. P. J. H. Bosman and P. T. Beurskens, *J. Cryst. Mol. Struct.*, *2*, 23 (1972). R = C_6H_5CN, X = Cl, Br: M. Massaux and M. T. Le Bihan, *Acta Cryst.*, *B32*, 1586. (1976). *Acta Cryst.*, *B32*, 2032 (1976). R = Pyridine, X = Cl: J. A. Campbell, C. L. Raston and A. H. White, *Austr. J. Chem.*, *30*, 1937 (1977).
7 B. N. Storhoff and H. C. Lewis Jr, *Coord. Chemistry Rev.*, *23*, 1 (1977). M. Massaux, M. T. Le Bihan and R. Chevalier, *Acta Cryst.*, *B33*, 2084 (1977).
8 Z. Rappoport, 'The Chemistry of the Cyano Group', Interscience, New York (1970).
9 M. Massaux, G. Ducreux, R. Chevalier and M. T. Le Bihan, *Acta Cryst.*, *B34*, 1863 (1978).
10 M. Massaux, M. T. Le Bihan and R. Chevalier, *Acta Cryst.*, *B33*, 2084 (1977).
11 B. N. Storhoff and H. C. Lewis Jr, *Coord. Chemistry Rev.*, *23*, 1 (1977).
12 D. M. Gale, *J. Org. Chem.*, *35*, 970 (1970).
13 M. Bolte and J. Lemaire, *Nouv. J. Chim.*, *4*, 461 (1980).